Reconstructing and Tracking Network State from a Limited Number of Synchrophasor Measurements

Mevludin Glavic, *Senior Member, IEEE* Thierry Van Cutsem, *Fellow, IEEE*

***Abstract*—A method is proposed to reconstruct and track network state from a limited number of Phasor Measurement Unit (PMU) data. To deal with the resulting unobservability, the state with bus powers and generator voltages closest to previously estimated values is computed. Those values, treated as pseudo-measurements, are obtained from the last reconstructed state, in a recursive manner. The method involves solving an optimization problem with linear constraints. It is scalable insofar as it accommodates from a few PMUs up to configurations ensuring full network observability. Reconstruction of only a region is possible. These and other features are demonstrated on the Nordic32 test system, with synchronized phasors obtained from detailed time simulation of a situation evolving towards instability. Suitable choices of PMU location and pseudo-measurements are also discussed.**

***Index Terms*—PMU, synchronized phasor measurements, state estimation, state reconstruction, tracking, constrained least-squares.**

I. Introduction

Real-time tracking of system dynamics is one of the great promises of synchronized phasor measurement technology, if adequately supported by computational facilities, networking infrastructure and communications, and if available in sufficient number [1].

The Phasor Measurement Unit (PMU) is an accurate power system instrument able to gather, usually several, time synchronized voltage and current phasors (synchrophasors) at high rate (10-120 samples/second) [1]. These new technological solutions are available in present-day power systems but with scarce PMUs since the upgrade of existing power system infrastructures requires investments in these technologies and only incremental upgrades are realistic. Consequently, present-day power systems are far from having a PMU configuration that allows determining the whole system state from those measurements only [1], [2], and this situation is likely to hold true for quite some time.

A natural application of (scarce) PMUs is to enhance traditional state estimators [3], [4]. The latter run every few minutes and provide an "average snapshot" of the system state due to time skew in measurement set [3]. Synchronized phasor measurements collected in the time window of classical measurements can be used to reinforce the redundancy of the latter. From a practical viewpoint, it may be advantageous to post-process them separately in order to leave the state estimation software unchanged [5], [6]. Although more accurate, the estimated state is still an average snapshot, and it is produced at the slow rate of traditional state estimators.

Hence, one of the challenges in effective exploitation of existing or near-future PMU configurations is to "reconstruct" coherent system states from the available PMU data at a much higher rate than classical state estimation. The term "state reconstruction" is used here since the proposed approach shares the features of this general class of problems [7].

Research and development efforts have been devoted to using limited amounts of PMU data to increase situational awareness. For instance, a hybrid power flow model that combines PMU measurement data and power flow equations was introduced in [8]. A PMU morphed power flow approach was proposed in [9]; the approach starts from a solved power flow and proceeds by matching this known solution to the small number of PMU measurements. Reference [10] introduced the concept of interpolation of states of unobservable buses from observable ones, using the bus admittance matrix. Refs. [11], [12] also dealt with the effective use of a limited number of measurements. In [11] a traditional state estimation was formulated as regularized least squares problem, while [12] used a limited number of phasor measurements in harmonic state estimation and solves a constrained sparsity-maximization problem to this purpose.

References [13], [14] are more closely related to the approach presented in this paper. Reference [13] considered tracking network state using synchrophasors and relying on a Kalman filter assuming full system observability. A simple random-walk prediction model [15] is extended in order to detect abrupt changes in the system state. Reference [14] uses an improved measurement set in traditional state estimation, for improved performances during dynamic system conditions. This requires minimizing the weighted integrals, over certain time period and over a set of representative scenarios.

This paper extends the work in [16], [17]. It proposes to use PMU data to reconstruct and track the state of a sub-network. The overall objective is a tighter monitoring of the system evolution. Of particular interest is system evolution after a disturbance and, hence, the anticipation of possible cascading effects. The method relies on snapshots provided by PMUs but does not involve a model of system dynamic evolution. Thus, the concept is close to that of a "tracking state estimator" defined in the literature of the 70's [18], but using nowadays' technology. State reconstruction relies on synchrophasor measurements together with power and voltage pseudo-measurements. The latter yield the state closest to

M. Glavic (glavic@montefiore.ulg.ac.be) is visiting professor at the Dept. of Electrical Engineering and Computer Science of the University of Liège, Sart Tilman B37, B-4000 Liège, Belgium.

T. Van Cutsem (t.vancutsem@ulg.ac.be) is with the Fund for Scientific Research (FNRS), at the same department.

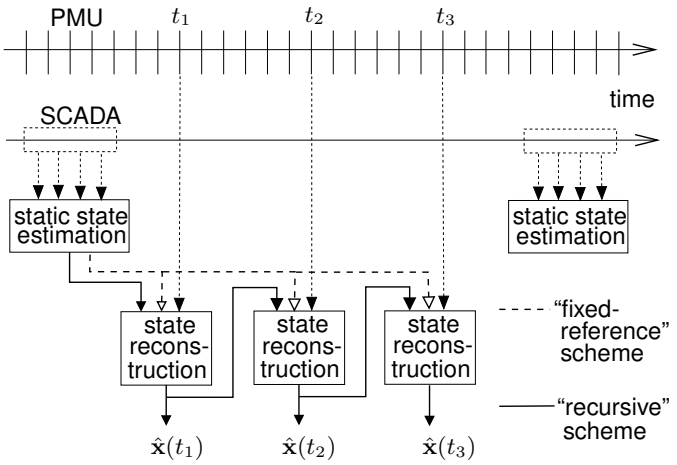

Fig. 1. Principle of state reconstruction

reference values, thereby removing the indeterminacy caused by the lack of PMU data. As sketched in Fig. 1, reference values stem either from the last run of a classical state estimator (variant shown with dashed lines) or from the last reconstructed state (shown with solid line).

The best location of a given number of PMU devices and the choice of pseudo-measurements are also discussed.

The remaining of the paper is organized as follows. The principle and the mathematical formulation are presented in Section II, simulation results in Section III, and concluding remarks in Section IV.

II. State reconstruction: principle and mathematical formulation

A. Network and measurement model

Let the network be modelled by the voltage-current relationships in rectangular coordinates:

$$\mathbf{G}\mathbf{v_x} - \mathbf{B}\mathbf{v_y} - \mathbf{i_x} = \mathbf{0} \tag{1a}$$

$$\mathbf{B}\mathbf{v_x} + \mathbf{G}\mathbf{v_y} - \mathbf{i_y} = \mathbf{0} \tag{1b}$$

where $\mathbf{v}_x$ and $\mathbf{v}_y$ are the real and imaginary parts of the vector of complex bus voltages, $\mathbf{i}_x$ and $\mathbf{i}_y$ the real and imaginary parts of the vector of complex currents injected at the buses, $\mathbf{G}$ and $\mathbf{B}$ the real and imaginary parts of the bus admittance matrix. The dimension of $\mathbf{v}_x, \mathbf{v}_y, \mathbf{i}_x$ and $\mathbf{i}_y$ is N, the number of system buses. For compact notation, these vectors are grouped into the single state vector of dimension $4N$:

$$\mathbf{x} = \begin{bmatrix} \mathbf{v}_x \\ \mathbf{v}_y \\ \mathbf{i}_x \\ \mathbf{i}_y \end{bmatrix} \tag{2}$$

The objective is to compute the system state that best fits a number of phasor measurements, provided by PMUs. The voltage and current phasors are decomposed into their rectangular components, further grouped into a measurement vector denoted $\mathbf{z}$. The latter relate to $\mathbf{x}$ through:

$$\mathbf{z} = \mathbf{A}\,\mathbf{x} + \boldsymbol{\omega} \tag{3}$$

where $\boldsymbol{\omega}$ is an (unknown) noise vector. For a bus voltage or a bus current measurement, the two rows of matrix $\mathbf{A}$ are unit vectors with the nonzero entries corresponding to the measured voltage or current component. For a branch current measurement, each of the two rows of matrix $\mathbf{A}$ has four nonzero terms, corresponding to the rectangular components of the voltages at the two ending bus of the branch.

Furthermore, the "infinitely accurate" information of zero current injections at "transit" buses without load or generation connected is modeled as:

$$\mathbf{C}\,\mathbf{x} = \mathbf{0} \tag{4}$$

where each row of $\mathbf{C}$ is a unit vector with the nonzero entry corresponding to the bus current component of concern.

B. Underdetermined least-square estimation

A conventional weighted least square estimation would consist of solving the constrained optimization problem:

$$\begin{aligned} \min_{\mathbf{x}} \quad & (\mathbf{z}-\mathbf{A}\mathbf{x})^{\mathbf{T}}\,\mathbf{W}\,(\mathbf{z}-\mathbf{A}\mathbf{x}) \\ \text{subject to} \quad & (1) \text{ and } (4) \end{aligned} \tag{5}$$

where $\mathbf{W}$ is a weighting matrix. The main issue, however, is that the PMU configuration provides scarce measurements which do not make the system observable, as discussed in the Introduction. Hence, the above problem is underdetermined, and there is an infinite number of states $\mathbf{x}$ satisfying the available measurements.

Regularization is a standard engineering approach to solve this type of indeterminacy [19], [20]. As stated in [19], it consists of including knowledge about the particular system and additional information about the unknowns in order to get a useful solution of an underdetermined system. The most straightforward information is an estimate of $\mathbf{x}$, in which case the distance to this estimate (in the L_0, L_1 or L_2-norm sense) is added to the objective (5) to remove indeterminacy. Examples of application to power system problems are presented in [11] for static and in [12] for harmonic state estimation.

The approach proposed in this paper bears the spirit of regularization but does not rely on the state vector itself, for reasons explained in the sequel. Instead, the sought state vector minimizes the squared distance to a reference in the space of variables $\mathbf{y}$ offering better predictability than the state vector itself. Thus, the optimization problem (5) is modified into:

$$\begin{aligned} \min_{\mathbf{x}} \quad & (\mathbf{z}-\mathbf{A}\mathbf{x})^{\mathbf{T}}\,\mathbf{W}\,(\mathbf{z}-\mathbf{A}\mathbf{x}) \\ & + \left[\mathbf{y}^{ref} - \mathbf{f}\,(\mathbf{x})\right]^{\mathbf{T}}\,\mathbf{W}_y\left[\mathbf{y}^{ref} - \mathbf{f}\,(\mathbf{x})\right] \\ \text{subject to} \quad & (1) \text{ and } (4) \end{aligned} \tag{6}$$

where $\mathbf{W}_y$ is a weighting matrix, $\mathbf{y}^{ref}$ the vector of reference values for $\mathbf{y}$, and $\mathbf{f}(.)$ is the relationship between $\mathbf{y}$ and $\mathbf{x}$. The Euclidean distance has been chosen for coherency and since $\mathbf{y}^{ref}$ and $\mathbf{z}$ are going to be treated similarly.

C. Choice of reference variables and PMU locations

The obvious choice for $\mathbf{y}$ would be the last known values of bus voltages. However, the best circumstance for tracking the

network state is after a disturbance. In the time interval that follows, bus complex voltages may undergo large variations (the more severe the disturbance, the larger the deviations).

The active and reactive powers consumed by loads also change, owing to their sensitivity to voltage and frequency, but this change is usually in the order of a few percents. Hence, load powers are good candidate references. A similar conclusion was drawn in [21], about the performance of traditional state estimation after a massive loss of measurements: using power injections at buses of the affected area as pseudo-measurements offers stable and acceptable results.

For a generator under Automatic Voltage Regulator (AVR) control, as long as its reactive power limits are not reached, the regulated voltage (magnitude) undergoes little changes. It is thus also a good candidate reference value. To identify the switching of a generator under field current limit, the techniques in [23] can be re-used.

The powers produced by generators vary comparatively more under the effect a disturbance, owing to their participation in voltage and frequency control. For instance, the outage of a transmission line induces changes in the reactive power of nearby voltage-controlled generators. Thus, it makes sense to monitor more closely these more "volatile" powers. This suggests placing PMUs to monitor generator powers.

With the above choice of reference values, $\mathbf{y}^{ref}$ involves active and reactive powers and (generator) voltages. Assuming diagonal matrices for $\mathbf{W}$ and $\mathbf{W}_y$, and detailing the components of $\mathbf{f}$, the objective (6) can be rewritten as:

$$\begin{aligned}\min_{\mathbf{x}} \quad & \sum_{i=1}^{m} w_i \left(z_i - \mathbf{a}_i\mathbf{x}\right)^2 \\ + \quad & \sum_{j=1}^{m_P} w_{Pj} \left(P_j^{ref} - v_{xk}i_{xk} - v_{yk}i_{yk}\right)^2 \\ + \quad & \sum_{j=1}^{m_Q} w_{Qj} \left(Q_j^{ref} - v_{yk}i_{xk} + v_{xk}i_{yk}\right)^2 \\ + \quad & \sum_{j=1}^{m_V} w_{Vj} \left((V_j^{ref})^2 - v_{xk}^2 - v_{yk}^2\right)^2 \end{aligned} \tag{7}$$

in which k refers to the bus where the reference value is specified, and $\mathbf{a}_i$ is the i-th row of $\mathbf{A}$.

At this point, the approach can receive another interpretation: the P_j^{ref}, Q_j^{ref} and $(V_j^{ref})^2$ values can be viewed as *pseudo-measurements complementing phasor measurements to make the system observable*.

In standard state estimation, it is customary to add pseudo-measurements to deal with unobservable situations. Usually, the minimal number of pseudo-measurements sufficient to restore observability is considered. The main motivation is to avoid corrupting with data of lower accuracy the observable part of the system, typically a large fraction of the latter. The added pseudo-measurements are critical; hence, the weights assigned to them have no impact on the solution.

The situation tackled in this work is completely different. Here, zero injection and synchrophasor data leave most of the system unobservable. Pseudo-measurements are added for regularization purposes. In this respect, any information available on the system state should be exploited. This leads to including as many pseudo-measurements as possible in the objective (7). Being redundant with the PMU data, the pseudo-measurements must be assigned proper weights, lower than those of the more accurate synchrophasor measurements. The weights should lead to a reconstructed state closely matching PMU data, while leaving larger residuals on pseudo-measurements.

More research is needed to identify an "optimal" (not necessarily diagonal) weighting matrix $\mathbf{W}_y$. This issue is outside the scope of the paper. However, already accurate reconstructed states have been obtained assuming "reasonable" values for w_{Pj}, w_{Qj} and w_{Vj} in (7).

Finally, an important choice is the time to which the reference values relate. Two options can be considered:

1) *fixed-reference:* the reference values are estimates stemming from the last execution of a standard state estimator. This variant is shown with dashed lines in Fig. 1. Clearly, it does not take into account the changes in operating conditions that have occurred in the meantime;
2) *recursive:* use the last reconstructed values, i.e. values computed by the same procedure, from the previous sample of phasor measurements. The estimates provided by a standard state estimator are used only in the first state reconstruction that follows that state estimation. This variant is shown with solid lines in Fig. 1. It allows to adjust to changing operating conditions.

The tests reported in Section III clearly show that the recursive scheme is to be preferred for its higher accuracy.

D. Solving the optimization problem

1) Newton scheme: The objective (7) is minimized with respect to $\mathbf{x}$, under the equality constraints (1, 4). In this optimization problem, all constraints are linear; nonlinearity is present in the objective only. Moreover, the latter being a multivariate polynomial function that can be expressed as a Sum-Of-Squares (SOS), it is SOS-convex, and hence convex [22]. This brings advantages such as global optimum and efficient and reliable numerical solution. The $\mathbf{G}$, $\mathbf{B}$ and $\mathbf{A}$ matrices are very sparse.

The problem being rewritten in compact form as:

$$\min_{\mathbf{x}} f(\mathbf{x}) \tag{8a}$$

$$\text{subject to : } \mathbf{Dx} - \mathbf{b} = \mathbf{0} \tag{8b}$$

the Karush-Kuhn-Tucker first-order optimality conditions are:

$$\frac{\partial f}{\partial \mathbf{x}} + \boldsymbol{\lambda}^T\mathbf{D} = \mathbf{0} \tag{9}$$

$$\mathbf{Dx} - \mathbf{b} = \mathbf{0} \tag{10}$$

where $\boldsymbol{\lambda}$ is the vector of Lagrange multipliers (or dual variables) associated with the linear constraints (8b). The dimension of $\boldsymbol{\lambda}$ is c, the number of constraints (8b).

Equations (9) and (10) are nonlinear equations to be solved with respect to $\mathbf{x}$ and $\boldsymbol{\lambda}$. The Newton method is used to this purpose. Let $\mathbf{x}^k$, $\boldsymbol{\lambda}^k$ and $\left(\frac{\partial f}{\partial \mathbf{x}}\right)^k$ be the values of $\mathbf{x}$, $\boldsymbol{\lambda}$ and $\frac{\partial f}{\partial \mathbf{x}}$

at the k-th iteration. The variables are updated according to:

$$\begin{bmatrix} \frac{\partial^2 f}{\partial \mathbf{x}^2} & \mathbf{D}^T \\ \mathbf{D} & \mathbf{0} \end{bmatrix} \begin{bmatrix} \mathbf{x}^{k+1} - \mathbf{x}^k \\ \boldsymbol{\lambda}^{k+1} - \boldsymbol{\lambda}^k \end{bmatrix} = - \begin{bmatrix} \left(\frac{\partial f}{\partial \mathbf{x}}\right)^k + \left(\boldsymbol{\lambda}^k\right)^T \mathbf{D} \\ \mathbf{D}\mathbf{x}^k - \mathbf{b} \end{bmatrix} \tag{11}$$

The size of this system is $4N + c$. Note that the coefficient matrix is symmetric. It also very sparse due to the sparsity of $\frac{\partial^2 f}{\partial \mathbf{x}^2}$ and $\mathbf{D}$, and the presence of the zero submatrix.

A "dishonest" scheme is used, in which the coefficient matrix is updated and factorized as rarely as possible. When this takes place, only the $\frac{\partial^2 f}{\partial \mathbf{x}^2}$ sub-matrix changes. Furthermore, the positions of the nonzero entries of this matrix remain unchanged for many successive state reconstructions. Hence, optimal ordering (based on the matrix sparsity pattern) can be performed very infrequently.

Last but not least, in tracking mode, $\mathbf{x}$ and $\boldsymbol{\lambda}$ are initialized at their values computed at the previous state reconstruction. In a full re-initialization, all components of $\mathbf{v}_x$ are set to one, those of $\mathbf{v}_y$, $\mathbf{i}_x$ and $\mathbf{i}_y$ to zero and those of $\boldsymbol{\lambda}$ to one.

2) Discussion: An alternative would consist of expressing currents as functions of voltages, using (1), and substituting the resulting expressions in the objective (7) and constraints (4). This would remove (1) from the set of equality constraints, thereby reducing the size of the system (11). However, at the same time, it would make the objective more nonlinear.

One motivation for retaining the currents as variables is the availability of current phasor measurements, easily handled in (3). Furthermore, using Newton method, any linear equation in (10) is satisfied after the first iteration. Thus, no degradation of convergence is to be expected when adding linear equality constraints such as (1). Finally, the coefficient matrix in (11) is larger but it is also much sparser.

Nevertheless, the above algorithm is one among several possible choices. It was found very satisfactory, particularly in tracking mode, which is a distinctive feature of state reconstruction.

III. Simulation results

A. Test system and scenario

The simulation results have been obtained with the Nordic32 test system, already used in [23]. The one-line diagram of this 74-bus, 102-branch, 20-machine system is shown in Fig. 2. A detailed time simulation under phasor approximation has been performed to obtain the "exact" system evolution after a severe disturbance. The simulated model involves:

- a detailed representation of synchronous generators;
- generic models for AVRs, excitation systems, prime movers and speed governors;
- Load Tap Changers (LTCs) controlling with various delays the voltages at distribution buses (shown without number in Fig. 2) where loads are connected;
- exponential model for load power variation with voltage;
- OverExcitation Limiters (OELs) with either fixed- or inverse-time response.

In order to test the method in stringent conditions, successive states of the network undergoing long-term voltage instability are reconstructed. A three-phase fault is applied

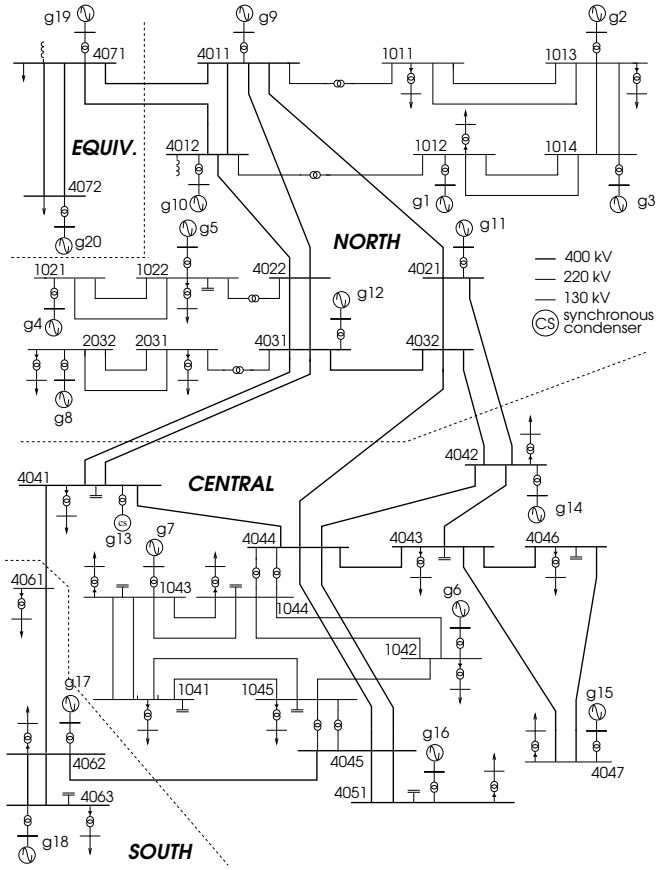

Fig. 2. Nordic-32 test system

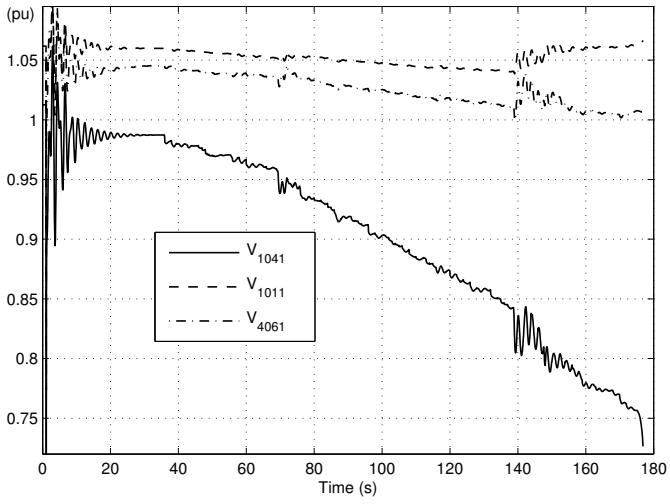

Fig. 3. Evolution of voltage magnitudes at several buses

on line 4032-4044 at $t = 1$ s, and is cleared by opening that line. The voltage magnitude at bus 1041, located in Central region (see Fig.2), is shown in Fig. 3. The progressive degradation of operating conditions is caused by LTCs and OELs, while the system eventually collapses when machine g6 loses synchronism.

The model processed in state reconstruction involves the 52 transmission and generator buses; distribution buses are not considered. The loads are thus the powers entering the dis-

tribution transformers. The tap changes in these transformers are neither known nor modeled in state reconstruction. On the other hand, the line tripping due to fault clearing is assumed to be know and reflected in the bus admittance matrix.

Figure 3 also provides the evolution of voltages at buses 1011 and 4061, located in North and South regions, respectively. They show that those regions are much less impacted. Therefore, to demonstrate the ability of the method to reconstruct the state of only a sub-system, the focus will be on the 19 buses of Central region, together with the 5 outside, directly connected buses, namely 4021, 4031, 4032, 4061 and 4062. This is referred to in the sequel as "region of interest".

PMUs have been assumed in that region. In accordance with the considerations of Section II.C, they are located at generator buses, namely g6, g7, g11, g14, g15, and g16. Each PMU measures two phasors: voltage and current injected by the generator. Only two channels per PMU have been considered, to avoid too rich a coverage of this small system.

PMU data have been obtained by sampling at regular time interval the rectangular components of voltages and currents given by time simulation, and adding to each component a Gaussian noise $N(0,\sigma)$ with $\sigma = 0.0033$ pu. Thus the simulated synchrophasor measurements are affected by sensor noise as well as by transients.

Ten buses have zero injections (namely buses 4011, 4012, 1014, 1021, 4022, 4021, 4031, 4032, 4044 and 4045).

Those 12 phasor measurements and 10 zero injections leave the whole system unobservable. Let us stress that the region of interest is also unobservable. The following pseudo-measurements have been considered: active and reactive powers of all 22 loads, active power and bus voltage of the 14 generators not provided with PMUs. Thus, there is a total of $2 \times (12 + 10 + 22 + 14) = 116$ measurements to determine the $2 \times 52 = 104$ voltage components. A diagonal matrix $\mathbf{W}_y$ has been considered, each diagonal term being the squared inverse of a "reasonable" standard deviation set to 0.016 pu for voltages and 0.033 pu for powers.

The fixed-reference reconstructions and the first recursive reconstruction use as pseudo-measurements the values obtained from the last run of a classical state estimator. The latter have been simulated by adding to the exact voltages and powers a Gaussian noise with standard deviation three times larger than that of the PMU data.

B. Overall accuracy of state reconstruction

Figure 4 shows the exact and reconstructed evolutions, over the last 120 seconds, of the voltage magnitude at bus 1041. The latter is not measured through PMU, just reconstructed. The accuracy of recursive state reconstruction, performed every one second, is noteworthy, even during the transients. Fixed-reference reconstruction, performed at the same rate, is comparatively less accurate, particularly after $t = 140$ s. This corresponds to g15 going under field current limit, soon followed by g16. The resulting voltage drops (see Fig. 3) cause a decrease of load power, and hence generation rescheduling according to primary frequency control. This system-wide change is not captured by the fixed-reference reconstruction while recursive reconstruction adapts itself remarkably well.

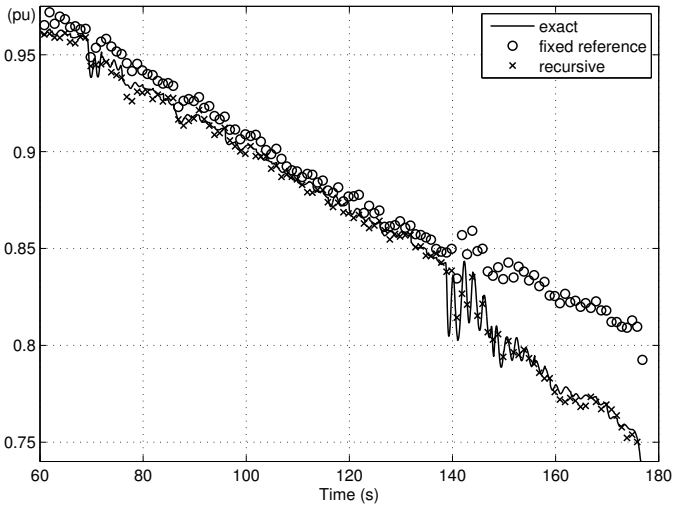

Fig. 4. Exact and reconstructed magnitude of voltage at bus 1041

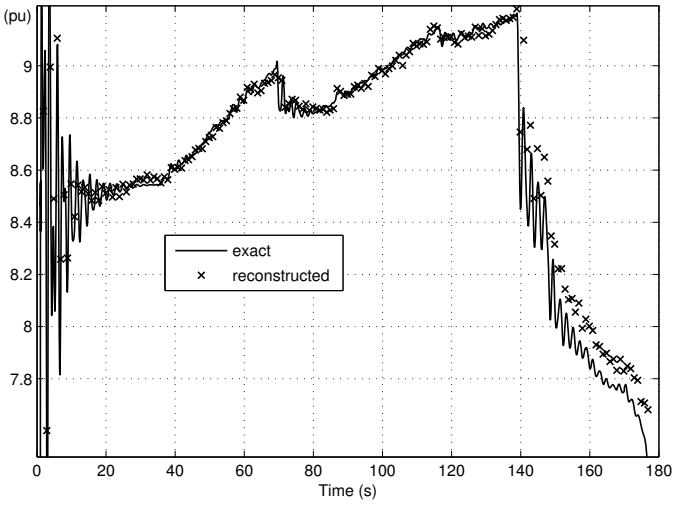

Fig. 5. Exact and reconstructed current in line 4032-4042

One possible usage of state reconstruction is the anticipation of near-future system evolution and cascading effects of disturbances. The currents in important transmission lines are of particular interest. An example is provided in Fig. 5, comparing the exact and reconstructed values of the current (magnitude) in line 4032-4042, linking Central and North regions as the tripped line. Very good accuracy is observed, with a maximum error of 0.15 pu (1.74% of pre-fault current) a little before collapse. Note that this accuracy is obtained with PMUs located on one side of the line only (in Central region).

Figure 6 shows similar results for the active power consumed by the load at bus 1041. The curve shown with solid line reveals large excursions of that power under the effect of rotor angle swings and load tap changers. Thus the system and the scenario considered in this paper offer a good testbed for checking the validity of using past bus power injection values for state reconstruction. The better performance of recursive reconstruction is further confirmed by the other curves, as well as by Table I giving the average and maximum reconstruction errors of respectively the voltage magnitude, the active and

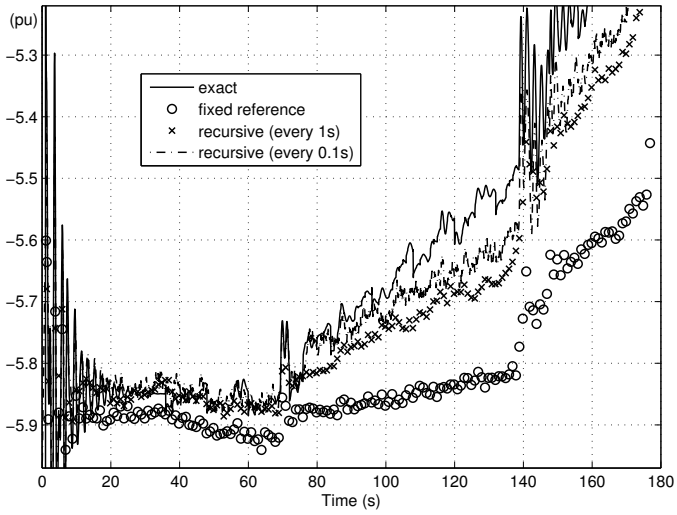

Fig. 6. Exact and reconstructed active power of load at bus 1041

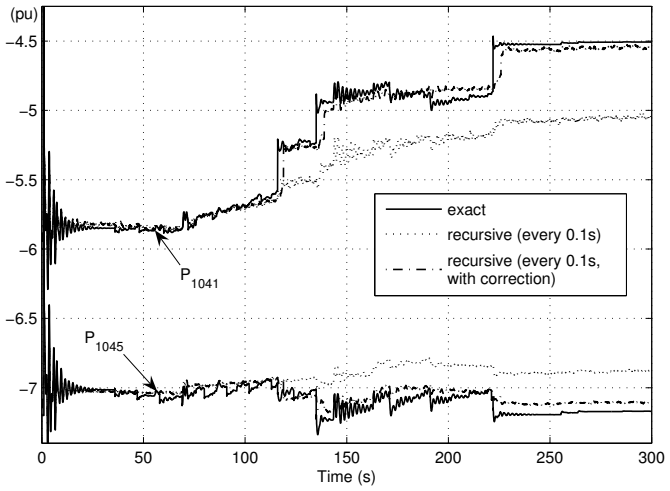

Fig. 7. Exact and reconstructed voltage at bus 1041 with load shedding

TABLE I
RECONSTRUCTION ERRORS AT BUS 1041

reference	period	average / maximum error on		
		V (pu)	P (pu)	Q (pu)
fixed	1 s	0.017 / 0.070	0.186 / 0.370	0.077 / 0.140
recursive	1 s	0.006 / 0.008	0.074 / 0.140	0.037 / 0.055
recursive	0.1 s	0.002 / 0.005	0.043 / 0.080	0.016 / 0.026

the reactive power of bus 1041.

Next, we report on a case where the assumption that load powers do not change much from one state reconstruction to the next meets its limits.

To stabilize this voltage unstable system, load was shed at bus 1041 in three successive steps. The corresponding results are given in Fig. 7, where the load curtailments are easily identified from the three jumps in the (solid-line) curve of the power at bus 1041. This significant modification of a *single* load creates some sort of distortion among the loads. Hence, after the first load shedding, a discrepancy appears between exact and reconstructed powers (see dotted lines in Fig. 7), especially at bus 1041 where curtailment took place. That discrepancy can be explained by the absence of information about the sudden load change in the pseudo-measurements; apparently, the available phasor measurements do not either reflect this event.

The dash-dotted curves in the same figure correspond to simulations where SCADA measurements of the active and reactive powers at bus 1041 are assumed to be received four seconds after each load shedding. These data are used as pseudo-measurements in the first state reconstruction following their (assumed) receipt. From there on, state reconstruction proceeds in recursive mode as already explained. The curves clearly show the benefit of this pseudo-measurement update. Even if it takes place at a few isolated time instants, it allows state reconstruction to reset and track the exact evolution more closely.

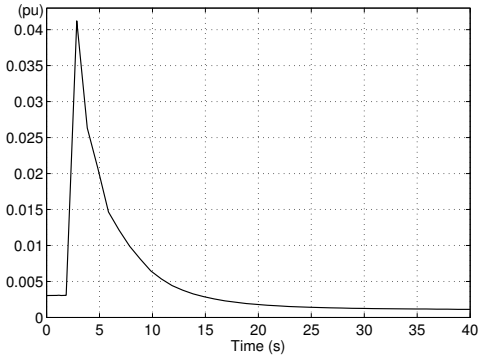

Fig. 8. Difference between current evolutions reconstructed with and without noise on the initial pseudo-measurements values

C. Effect of state reconstruction rate

Figures 6 and 7, as well as Table I also show the results of reconstruction performed at higher rate, namely every 0.1 s. The tracking capability is better. However, running every 1 s offers already satisfactory results, while being computationally less demanding. Recursive reconstruction every 1 s is thus considered in the remaining of this paper.

D. Robustness with respect to errors on the initial state

The method is robust with respect to errors on the initial system state. This is illustrated in Fig. 8 relative to the same current as Fig. 5. The plot shows the difference between reconstructed currents with and without noise on the pseudo-measurement values relative to the initial, pre-disturbance state. The impact of noise is observed during some 20 s after the disturbance, after which it is negligible.

E. Impact of pseudo-measurement configuration

Pseudo-measurements are added for regularization purposes. In this respect any information on the system state should be exploited. The results of this section support the

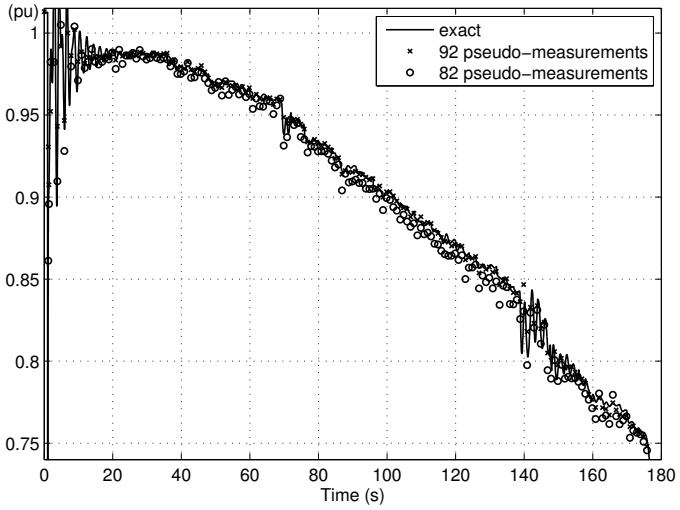

Fig. 9. Voltage at bus 1041 for two pseudo-measurement configurations

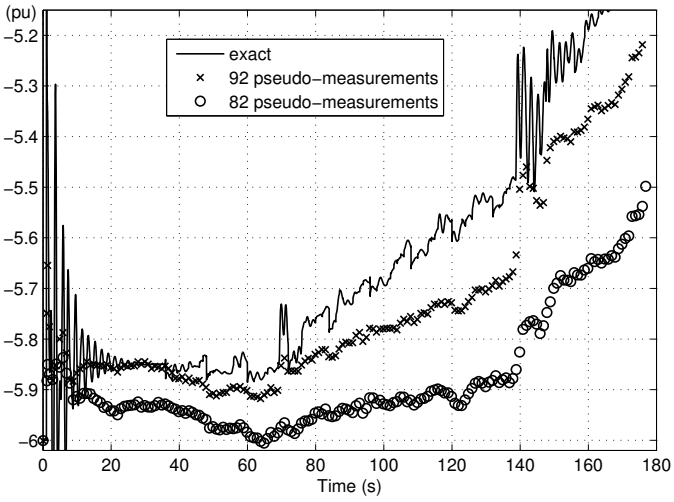

Fig. 10. Active power at bus 1041 for two pseudo-measurement configurations

statement that it is desirable to include as many pseudo-measurements as possible. To this purpose, two pseudo-measurement configurations are compared:

- the configuration detailed in Section III.A, and used in all results shown so far. It includes 92 pseudo-measurements, which corresponds to 12 pseudo-measurements more than the number strictly needed to restore observability;
- the same with the active and reactive power pseudo-measurements removed at five load buses (namely buses 1011, 1012, 2031, 4043, and 4061), thus leading to a set of 82 pseudo-measurements.

The corresponding reconstructed evolutions of the voltage magnitude and active power at bus 1041 are given in Figs. 9 and 10, respectively. The voltage magnitude is relatively little affected, while for the active power the impact of using less pseudo-measurements is clear. Although four of the five removed load pseudo-measurements are located outside the region of interest, it impacts the accuracy of state reconstruction in this region. This observation holds true for other buses in the region of interest (except those monitored by PMUs).

F. Evaluating PMU configurations

The results of this section show the impact of PMU configuration on reconstruction accuracy and support the intuitive reasoning of Section II.C that generators should be monitored. The accuracy is assessed using the average Euclidean distance between the exact and reconstructed voltage evolutions:

$$d_k = \sqrt{\frac{1}{N_b}\sum_{i=1}^{N_b} ||\bar{V}_i^{ex}(k) - \bar{V}_i^{rec}(k)||^2} \qquad (12)$$

where $\bar{V}_i^{ex}(k)$ denotes the exact complex voltage at bus i at sampling time k, $\bar{V}_i^{rec}(k)$ is the corresponding reconstructed value and the sum extends over the buses in the region of interest ($N_b = 24$ in our case). At each time k, reconstructed voltage phase angles are shifted (all by the same amount) so that the phase angle at a reference bus coincides with the phase angle of the exact voltage at that bus. Thus, if reconstructed and exact voltage phasors differ by a rotation only, d_k is zero.

TABLE II
RECONSTRUCTION ERROR FOR DIFFERENT PMU CONFIGURATIONS

n_{pmu}	N_c	best location	d (pu)
1	8	g15	0.1551
2	28	g11, g15	0.0348
3	56	g11, g15, g16	0.0258
4	70	g7, g11, g15, g16	0.0222
5	56	g7, g11, g14, g15, g16	0.0213
6	**28**	**g6, g7, g11, g14, g15, g16**	**0.0142**
7	8	g6, g7, g11, g13, g14, g15, g16	0.0076
8	1	g6, g7, g11, g12, g13, g14, g15, g16	0.0068
10	1	g6, g16, 1043, 1045, 4021, 4031, 4041, 4042, 4045, 4047	0.0061

For easier comparisons, the following average distance is also considered:

$$d = \frac{1}{N_s}\sum_{k=1}^{N_s} d_k \qquad (13)$$

where N_s is number of sampled times.

First, simulations were conducted to identify the best generator buses to provide with a given number of PMUs. Among the above mentioned 24 buses, there are 8 candidate generator buses, namely: g6, g7, g11, g12, g13, g14, g15, and g16 (see Fig. 2). For a given value of n_{pmu}, all N_c possible combinations of n_{pmu} PMUs among the 8 buses were tested and the one yielding the smallest value of d was identified. Each PMU has 2 channels and measures one bus voltage and one generator current phasor.

Table II shows N_c, d and the best combination of generator buses, for n_{pmu} varying from 1 to 8, while Fig. 11 shows the corresponding evolutions of d_k with time k.

The table and the figure also include results obtained with a configuration of 10 multi-channel PMUs ensuring observability of the region of interest. Each PMU measures the voltage of a different bus and all currents leaving that bus. This leads to a total of 10 voltage and 38 current phasors. The choice of the buses has been optimized to obtain full observability at minimum PMU cost. The method presented in [24] was used,

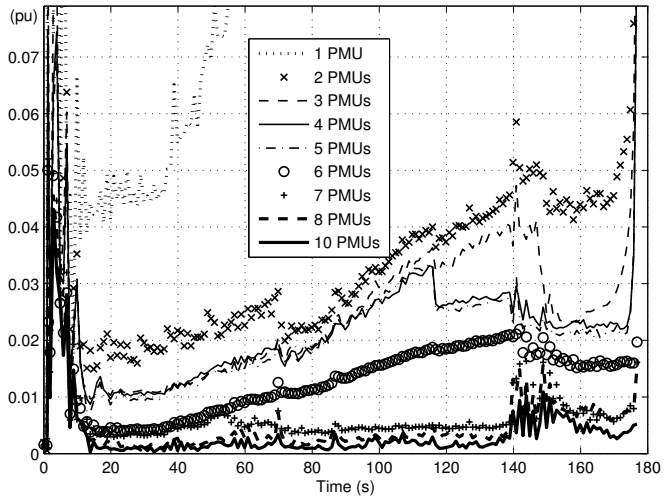

Fig. 11. Euclidean distance d_k for the PMU configurations in Table II

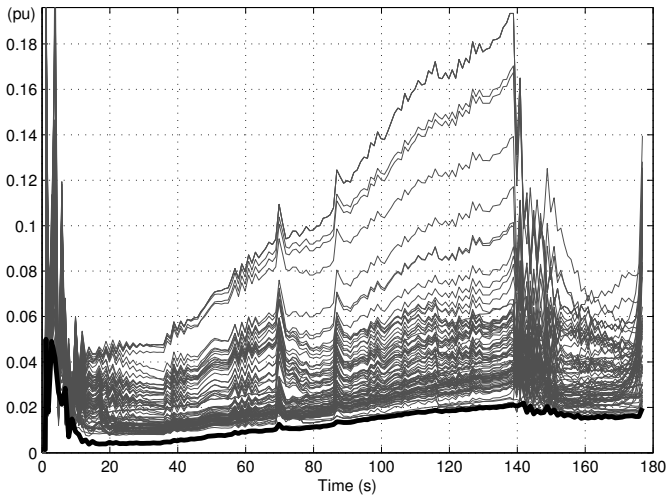

Fig. 12. Average Euclidean distance with 6 PMUs

combining a graph-theoretic procedure with modified bisection search and a simulated annealing method.

As expected, the curves show that accuracy improves as n_{pmu} increases. For n_{pmu} comprised between 1 and 5, the curves reveal a progressive drift of reconstructed voltages with respect to exact values. However, even with as few as 2 PMUs, the accuracy is quite good over the first 70 seconds. For n_{pmu} larger than 6, the accuracy is excellent over the whole system evolution, with a slight degradation after $t = 140$ s. At that time, however, bus voltages are already very depressed, as can be seen from Fig. 3.

Figure 11 shows that the 8- and 10-PMU configurations bring little improvement with respect to the 7-PMU configuration. This result is even more remarkable that the 7- and 8-PMU configurations do not ensure observability of the region of interest. The figure also shows that the 6-PMU configuration offers some compromise between PMU cost and accuracy. This motivated the choice of that configuration for producing the results presented in previous sections.

Next, the so identified 6-PMU configuration was compared to a sample of 100 random configurations, each of them also involving n_{pmu} voltage phasors and n_{pmu} bus current phasors. The locations were chosen randomly among the 24 buses of interest, except at the 5 buses with zero injections. In Fig. 12, the evolution of d_k with time k is shown with bold line for the 6-PMU configuration and with grey lines for the 100 random configurations. This plot clearly confirms the higher accuracy obtained when monitoring generators.

The results of Table II and Fig. 11 also show that the method is *scalable*, in the sense that it accommodates PMU schemes ranging from a few locations up to configurations ensuring full network observability. As more and more PMUs will become available, the accuracy will progressively improve.

G. Performance of optimization procedure

Figure 13 shows the number of iterations (11) over the first 30 s of system evolution, when performing recursive reconstruction in the following conditions:

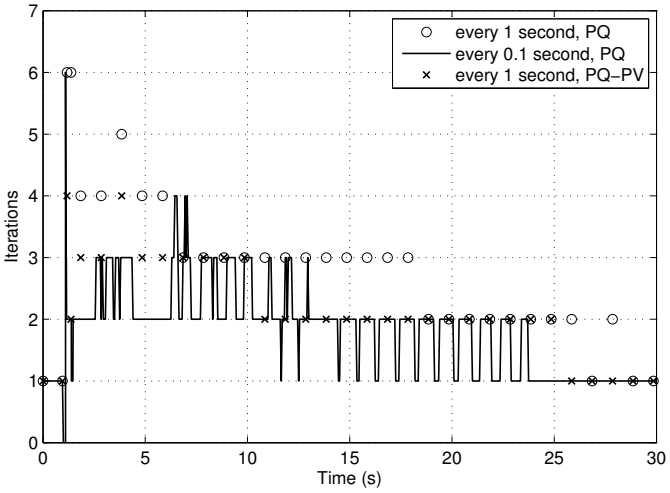

Fig. 13. Number of Newton iterations

- every 0.1 s, using the active power and voltage pseudo-measurements detailed in Section III.A;
- every 1.0 s, using the same pseudo-measurements;
- every 1.0 s, replacing reactive power by voltage magnitude pseudo-measurements at generator buses not provided with PMUs.

Iterations are stopped after all components of $\mathbf{x}$ and $\boldsymbol{\lambda}$ have been incremented by less than 10^{-5} pu. In steady-state conditions (for $t < 1$ s in the figure), a single iteration is performed.

It is seen that performing state reconstruction more frequently results in less iterations, because the last reconstructed state makes up a better initial guess for the next reconstruction. Also, less iterations are needed when specifying voltage (instead of reactive power) pseudo-measurements at generator buses. Expectedly, the computing times were also found shorter: around 33 % lower, on the average, compared to the case where only power pseudo-measurements are used.

It can happen that a phasor sample is taken during fault-on conditions. In this case, the iterations (11) either diverge or a large number of them are needed, but the solution should be

discarded (since the phasor and pseudo-measurements are not coherent). Setting a maximum number of iterations (for instance 10) is an effective way to recognize that reconstruction is run during abnormal conditions.

IV. Conclusion

A method has been proposed to track the changing state of a network, taking advantage of the synchronized phasor measurements available at much higher rate than classical state estimation measurements, but in limited number. The resulting unobservability is solved by complementing the PMU data with pseudo-measurements and zero injection information. The pseudo-measurements are power and voltage data at buses not provided with PMUs, obtained from the previous execution of the state reconstruction algorithm. The latter relies on a standard least square equality-constrained optimization.

The method is scalable in the sense that it accommodates PMU schemes ranging from a few locations up to configurations ensuring full network observability. Intuition together with simulation results suggest that, for higher accuracy, PMUs should be located at generator buses, while as many pseudo-measurements as possible should be used. This leads to some redundancy, which requires assigning lower weights to pseudo-measurements than to the more accurate synchronized phasor measurements.

Simulations results confirm the ability to reconstruct the system evolution with satisfactory accuracy. They also show the possibility of reconstructing the state of a region of interest only, provided with PMUs.

In between two classical state estimation runs, the network state can be reconstructed at various rates, the limitation being the time spent solving the constrained optimization. In tracking mode, however, the latter requires very few Newton iterations.

Among the aspects being currently investigated, let us quote:

- the assessment of performances in larger systems;
- the determination of "optimal" weighting for pseudo-measurements, although the encouraging results reported in this paper were obtained using "reasonable" values;
- the update of pseudo-measurements from SCADA measurements, when the latter are received, generalizing the procedure illustrated in Fig. 7;
- the exploitation of PMU data available in between successive state reconstructions;
- the possible use of state reconstruction results to improve standard state estimation.

References

[1] A. G. Phadke and J. S. Thorp, *Synchronized Phasor Measurements and their Applications*, Springer, New York, NY, 2008.

[2] A. G. Phadke, J. S. Thorp, and K. J. Karimi, "State Estimation with Phasor Measurements," *IEEE Trans. Power Syst.*, vol. 1, no. 1, pp. 233-238, Feb. 1986.

[3] A. Abur and A. Gomez Exposito, *Power System State Estimation: Theory and Implementation*, Marcel Dekker Inc., New York-Basel, 2004.

[4] A. Gomez-Exposito, A. Abur, P. Rousseaux, A. de la Villa Jean and C. Gomez-Quiles, "On the Use of PMUs in Power System State Estimation," *Proc. 17th Power System Computation Conference (PSCC)*, Stockholm, Sweden, Aug. 2011.

[5] M. Zhou, V. A. Centeno, J. S. Thorp, and A. G. Phadke, "An Alternative for Including Phasor Measurements in State Estimators," *IEEE Trans. Power Syst.*, vol. 21, no. 4, pp. 1930-1937, Nov. 2006.

[6] L. Vanfretti, J. H. Chow, S. Sarawgi, and B. Fardanesh, "A Phasor-Data-Based State Estimator Incorporating Phase Bias Correction," *IEEE Trans. Power Syst.*, vol. 26, no. 1, pp. 111-119, Feb. 2011.

[7] H. Kwakernaak and R. Sivan, *Linear Optimal Control Systems*, John Wiley & Sons, New York, 1972.

[8] N. Zhou, Z. Huang, J. Nieplocha, and T. B. Nguyen, "Wide-Area Situational Awareness of Power Grids with Limited Phasor Measurements," *Proc. Third International Conference on Critical Infrastructures (CRIS)*, Alexandria, VA, Sept. 2006.

[9] T. Overbye, P. Sauer, C. DeMarco, B. Lesieutre, and M. Venkatasubramanian, *Using PMU Data to Increase Situational Awareness*, Power System Engineering Research Center (PSERC) Report 10-16, Sep. 2010.

[10] R. F. Nuqui, "State Estimation and Voltage Security Monitoring Using Synchronized Phasor Measurements," PhD Thesis, Virginia Polytechnic Institute and State University, Blacksburg, VA, Jul. 2001

[11] M. C. de Almeida, A. V. Garcia, and E. N. Asada, "Requlalized Least Squares Power System State Estimation," *IEEE Trans. Power Syst.*, vol. 27, no. 1, pp. 290-297, Feb. 2012.

[12] H. Liao, "Power System Harmonic State Estimation and Observability Analysis via Sparsity Maximization," *IEEE Trans. Power Syst.*, vol. 22, no. 1, pp. 15-23, Feb. 2007.

[13] X. Bian, X. R. Li, H. Chen, D. Gan, and J. Qiu, "Joint Estimation of State and Parameter With Synchrophasors-Part I: State Tracking," *IEEE Trans. Power Syst.*, vol. 26, no. 3, pp. 1196-1208, Aug. 2011.

[14] M. Zima-Bockarjova, M. Zima, and G. Andersson, "Analysis of State Estimation Performance in Transient Conditions," *IEEE Trans. Power Syst.*, vol. 26, no. 4, pp. 1866-1874, Nov. 2011.

[15] A. S. Debs and R. E. Larson, "A Dynamic Estimator for Tracking the State of a Power System," *IEEE Trans. Power App. and Syst.*, vol. PAS-89, pp. 1670-1678, Sep./Oct. 1970.

[16] M. Glavic and T. Van Cutsem, "Investigating State Reconstruction from Scarce Synchronized Phasor Measurements," *Proc. IEEE PowerTech*, Trondheim, Norway, Jun. 2011.

[17] M. Glavic and T. Van Cutsem, "State Reconstruction from Synchronized Phasor Measurements," *Proc. IEEE Innovative Smart Grid Technologies (ISGT-Europe)*, Manchester, UK, Dec. 2011.

[18] R. Masiello and F. C. Schweppe, "A Tracking Static State Estimator," *IEEE Trans. Power App. and Syst.*, vol. PAS-90, pp. 1025-1033, Mar./Apr. 1971.

[19] P. C. Hansen, *Rank-Defficient and Discrete Ill-Possed Problems: Numerical Aspects of Linear Inversion*, Society of Industrial and Applied Mathematics (SIAM), 1998.

[20] C. L. Lawson and R. J. Hanson, *Solving Least Squares Problems*, Prentice-Hall, Englewood Cliffs, NJ, 1974.

[21] C. Gonzales-Perez and B. F. Wollenberg "Analysis of Massive Measurement Loss in Large-Scale Power System State Estimation," *IEEE Trans. Power Syst.*, vol. 16, no. 4, pp. 825-832, Nov. 2001.

[22] S. Prajna, A. Papachristodoulou, and P. A. Parrilo, "Introducing SOSTOOLS: A General Purpose Sum of Squares Programming Solver," *Proc. IEEE Control and Decision Conference (CDC)*, Pasadena, CA, Dec. 2002.

[23] M. Glavic, T. Van Cutsem, "Wide-Area Detection of Voltage Instability From Synchronized Phasor Measurements. Part II: Simulation Results," *IEEE Trans. Power Syst.*, Vol. 24, No. 3, pp. 1417-1425, Aug. 2009

[24] T. L. Baldwin, L. Mili, M. B. Boisen, and R. Adapa, "Power System Observability With Minimal Phasor Measurement Placement," *IEEE Trans. Power Syst.*, vol. 8, no. 2, pp. 707-715, May 1993.

Mevludin Glavic (M'04-SM'07) received the M.Sc. and Ph.D. degrees from the Univ. of Belgrade (Serbia) and Tuzla (Bosnia) in 1991 and 1997, respectively. He spent the academic year 1999-2000 with the Univ. of Wisconsin-Madison, as a Fulbright postdoctoral scholar. From 2001 to 2004, he has been a Senior Research Fellow at the Univ. of Liège. Since then he has been working as consultant for Deling-doo (Bosnia) in projects with AREVA (now ALSTOM) T&D (France), Suez Tractebel Eng. (Belgium), and Quanta Technology (USA). He is presently a visiting professor at the Univ. of Liège. His research interests are in power system dynamics, stability, security, optimization, and real-time control.

Thierry Van Cutsem (F'05) graduated in Electrical-Mechanical Engineering from the University of Liège (Belgium), where he obtained the Ph.D. degree and he is now adjunct professor. Since 1980, he has been with the Fund for Scientific Research (FNRS), of which he is now a Research Director. His research interests are in power system dynamics, stability, security, simulation and optimization, in particular voltage stability and security. He is currently vice-chair of the IEEE Power System Dynamic Performance Committee.